



HAL
open science

A new technique for increasing the sensitivity of marine DC-electrical resistivity acquisitions

Sérgio Palma Lopes, Philippe Côte

► To cite this version:

Sérgio Palma Lopes, Philippe Côte. A new technique for increasing the sensitivity of marine DC-electrical resistivity acquisitions. Near Surface Geoscience'20 (NSG 2020), EAGE, Dec 2020, Online Conference, France. pp.1-5, 10.3997/2214-4609.202020069 . hal-04533565

HAL Id: hal-04533565

<https://univ-eiffel.hal.science/hal-04533565v1>

Submitted on 22 Apr 2024

HAL is a multi-disciplinary open access archive for the deposit and dissemination of scientific research documents, whether they are published or not. The documents may come from teaching and research institutions in France or abroad, or from public or private research centers.

L'archive ouverte pluridisciplinaire **HAL**, est destinée au dépôt et à la diffusion de documents scientifiques de niveau recherche, publiés ou non, émanant des établissements d'enseignement et de recherche français ou étrangers, des laboratoires publics ou privés.

A new technique for increasing the sensitivity of marine DC-electrical resistivity acquisitions

Sérgio Palma Lopes and Philippe Côte
Université Gustave Eiffel, GERS-GeoEND

Summary

Direct current (DC) resistivity methods applied to geological mapping in marine environments can be very limited to shallow waters, depending on the resistivity contrast between seawater and the subsurface formations. In this paper, we introduce a new acquisition technique for increasing the signal sensitivity to geological targets, despite the presence of a seawater column. The suggested technique consists in the use of an insulating sheet laid directly on the electrode cable placed on the seafloor, an idea that had been previously patented. As a first step in assessing the efficiency of this approach, a synthetic study was carried out. Results are presented and briefly discussed. It is demonstrated that the increase in geoelectrical response sensitivity can be significant.

Introduction

Direct current (DC) resistivity methods applied to the investigation of underwater subsurface has drawn an increasing attention since the early 1980s (e.g. Lagabrielle 1983). The range of applications has become broader, including geotechnical engineering and geological mapping studies. Numerous interesting applications are listed in Tassis et al. (2020). Innovative DC-resistivity survey systems have been developed in the last decades (Goto et al. 2008, D'Eu et al. 2012). Although towed floating electrode arrays are quite popular, fixed electrode cables laid on the seafloor can be used when surveying a limited area, such as in straits or estuaries, and willing to achieve higher resolution images (Dahlin et al. 2014). However, depending on the resistivity contrast between the water column and the geological formations, marine surveys may be strongly limited to shallow waters (Tassis et al., 2020).

Here, we introduce a straightforward technique that consists in using an insulating sheet laid directly on the electrode line placed on the seafloor in order to mitigate the substantial loss in signal sensitivity due to the highly conductive water column. To our best knowledge, the patented idea (Lafont et al., 1991) has never been studied nor applied. The practical challenge of conceiving and implementing such an insulating sheet is out of the scope of the paper. The aim here is to evaluate the benefits in terms of signal sensitivity to geological targets, by means of forward numerical modelling. Our demonstration is based on two synthetic models. Results are presented and discussed before we conclude.

Numerical model features and insulating sheet implementation

In this section, we describe the common features of the 3D model used for all our numerical simulations. The model is a semi-infinite medium consisting in a rectangular cuboid divided into 3 domains with horizontal interfaces. The domains are homogeneous mediums representing (from top to bottom): a volume of seawater of thickness 30 m and resistivity ρ_w , a layer of sediments of thickness 10 m and resistivity ρ_s and finally the bedrock of quasi-infinite thickness 590 m and resistivity ρ_r . The horizontal dimensions of the model are 1200 m x 1200 m (Figure 1a). Boundary effects are assumed to be negligible. A Neumann condition is set on the top surface of the model (interface between seawater and air) with a zero current density flux across this face. The full electrode layout consists of a horizontal line of 31 point electrodes evenly spaced at an interval of 2 m. This electrode line of total length

$L = 60$ m is placed at the center of the model and is laid on the seafloor (Figure 1). The DC-resistivity forward problem is governed by Poisson's equation that we solve by means of finite element (FE) modelling under the Comsol Multiphysics 5.4 software. For each pair of transmitting electrodes, a DC excitation of arbitrary intensity I is imposed, and the electrical potential distribution V is solved for on all nodes of the model mesh. Subsequently, potential drops ΔV between receiving electrode pairs and transfer resistances $\Delta V/I$ can be retrieved.

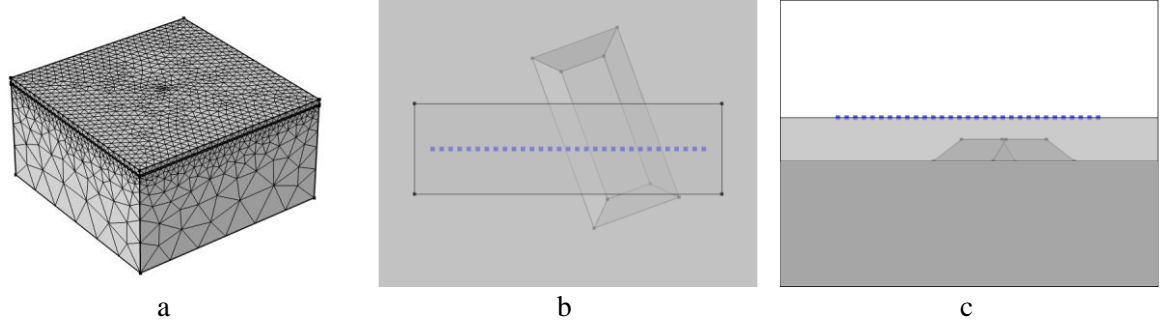


Figure 1 The synthetic model with a) full view of the 3D mesh, b) close-up view from above of the electrode line (blue points) with a rectangular insulating sheet on top (in black) and the geological target underneath and c) cross-section showing the electrodes at the bottom of the seawater column (in white) above the sediments (light grey), the target and the bedrock (dark grey).

Then for simulating the insulating sheet we generate a flat hollow volume laid directly on the electrode line (Figure 1b). This volume has a fixed thickness of 0.2 m in the model. Its length and width can be varied for the purpose of this study. We implement the same zero current density flux boundary condition across all 6 faces of the sheet. Therefore, it acts as a strictly insulating screen. The generated FE model discretization is based on an unstructured mesh of quadratic tetrahedral elements the sizes of which range from less than 0.04 m close to the electrodes to about 200 m on the external boundaries (Figure 1a). The number of degrees of freedom to be solved for ranges from $2 \cdot 10^5$ to 10^6 depending on the model features, and the numerical solutions convergence to errors less than 10^{-3} .

Fundamental effect of an insulating sheet

For the purpose of demonstrating our approach, the insulating sheet here is square of width W ranging from 0 to 40 m and only 4 of the most central electrodes equally spaced at an interval of $a = 4$ m are used. Studied electrode configurations are the Wenner- α and β arrays. Furthermore, the resistivities of the 3 domains aforementioned are set to the same value $\rho_w = \rho_s = \rho_r = 0.2 \Omega \cdot \text{m}$. Thus, a homogeneous half-space of 'seawater' is simulated in which the electrode line is submerged 30 m below the surface. In this case, a simple analytical expression exists for transfer resistances (Eq. 1):

$$\frac{\Delta V}{I} = \frac{\rho_w}{4\pi} \left[\left(\frac{1}{C_1 P_1} + \frac{1}{C'_1 P_1} - \frac{1}{C_2 P_1} - \frac{1}{C'_2 P_1} \right) - \left(\frac{1}{C_1 P_2} + \frac{1}{C'_1 P_2} - \frac{1}{C_2 P_2} - \frac{1}{C'_2 P_2} \right) \right] \quad (1)$$

with C_1 and C_2 the transmitting electrodes, C'_1 and C'_2 (virtual current sources) their respective mirror-images, the water/air interface being the plane of symmetry, and P_1 and P_2 the receiving electrodes.

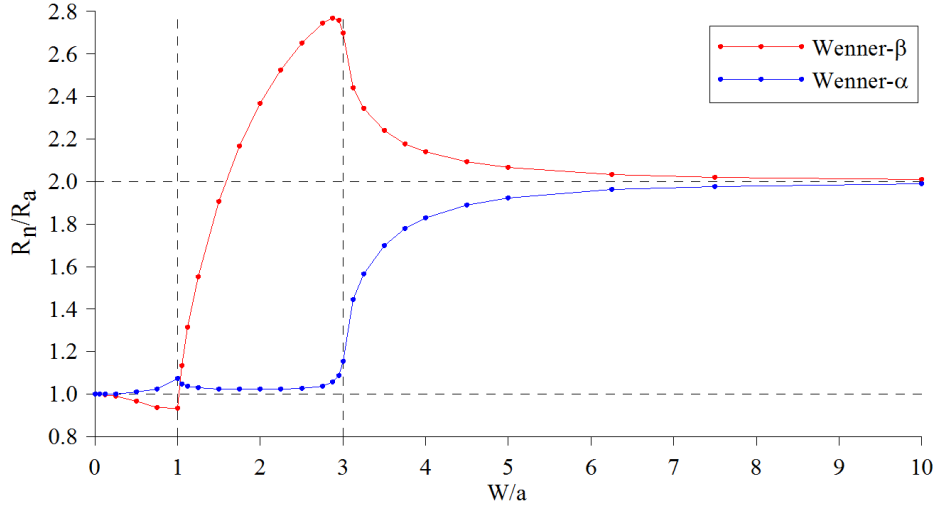


Figure 2 Effect of an insulating screen on the normalized responses of both the Wenner- α and β configurations, for the sheet width ranging from 0 to 10 times the electrode spacing a .

In Figure 2 we illustrate the effect of the insulating screen as a function of the screen width, for both Wenner- α and β electrode arrays with a constant electrode spacing $a = 4$ m. More specifically, we plot the normalized response R_n/R_a , where R_n is the numerically simulated transfer resistance in the presence of a screen and R_a the analytical one without a screen (Eq. 1), versus the screen width W normalized by the electrode spacing a . As expected, the R_n/R_a ratio tends to 1 as W tends to zero since the response is that of submerged electrode arrays in the absence of any screen. Moreover, the asymptotic behaviour for large widths ($W \gg a$) is that of electrode arrays on dry land (i.e. in the absence of a water column) which is very close to twice that of the submerged ones (Eq. 1) in the case of a 30 m thick water column. This twofold asymptotic trend is a good indicator for validating our insulating sheet simulation approach. In between these extremes, the Wenner- α and β responses are quite different and exhibit more complex trends. However, they both show pronounced variations in the vicinity of two specific values of W/a : when the sheet width equals the electrode spacing ($W = a$) and when the width equals the array length ($W = 3a$). We explain such behaviours and differences by the array-dependent sensitivity patterns as shown in 2D and on dry land by Dahlin and Zhou (2004), although this aspect would deserve dedicated calculations in a 3D aquatic environment.

Sensitivity to a geological target

Here we present a synthetic study of the signal sensitivity to a given geological target, depending on the size of the insulating sheet. The resistivities of the 3 domains are set to $\rho_w = 0.2 \Omega \cdot \text{m}$, $\rho_s = 20 \Omega \cdot \text{m}$ and $\rho_r = 2000 \Omega \cdot \text{m}$ respectively, thus simulating a 30 m seawater column over a two-layered medium with relatively high resistivity contrasts. The geological target is a rock dome inducing a local decrease in the depth to the bedrock. This dome is simulated by a hexahedron of horizontal dimensions 20 m x 40 m at its basis, of height 5 m (Figure 1c), of resistivity ρ_r and resting on the bedrock domain (Figure 1b and 1c). The target is not centered on the electrode line axis nor perpendicular to it, thus representing a fully 3D target. All 31 electrodes are used. The insulating sheet here is rectangular with a fixed length of 68 m (thus covering the whole electrode line) and a variable width W . We consider a series of 9 configurations of increasing ‘screen’ effect. First the ‘no screen’ configuration equivalent to the conventional marine acquisition. Then 7 configurations for values of W ranging from 1 m to 100 m. And finally the ‘no water’ configuration which is equivalent to an acquisition on dry land and also equivalent to a screen of ‘infinite’ length and width as previously shown. In each configuration, we compute the responses for a complete Wenner- α protocol (for all possible electrode spacings: $a = 2, 4, \dots, 20$ m) yielding 145 simulated data points. Although Wenner- α is often not the preferred array type for underwater acquisitions (Tassis et al. 2020), we use it for its simplicity. All these responses are noise-free and are calculated in two situations: with (‘target’ situation) and without (‘reference’ situation) the geological target. We then retrieve the transfer resistance ratios between these two situations. Such ratios yield the effect of the target on the responses (similar to the anomaly effect in Dahlin & Zhou,

2004). In Figure 3 we plot this target effect for two selected electrode spacings ($a = 6$ m and $a = 12$ m) as a function of the lateral position of the simulated measurements on the electrode line, and for each configuration. The target effect in the ‘no screen’ configuration is extremely close to 1, therefore showing that a conventional marine acquisition is clearly unable to detect the target. This is fully consistent with previous publications (e.g. Tassis et al. 2020) that assert a maximum water depth of about 10 m for geoelectrical surveys in marine environments. Then the target effect increases rapidly with the sheet width and starts stagnating for $W > L$. Indeed, the curves for $W = 60$ m and 100 m are almost identical. As expected, this increase depends on the electrode spacing. Therefore all the data acquired within a full DC-resistivity protocol are not impacted the same way. Although this falls out of the scope of this paper, we emphasize that available inversion software are unable to process such ‘screened’ data and a specific development is needed.

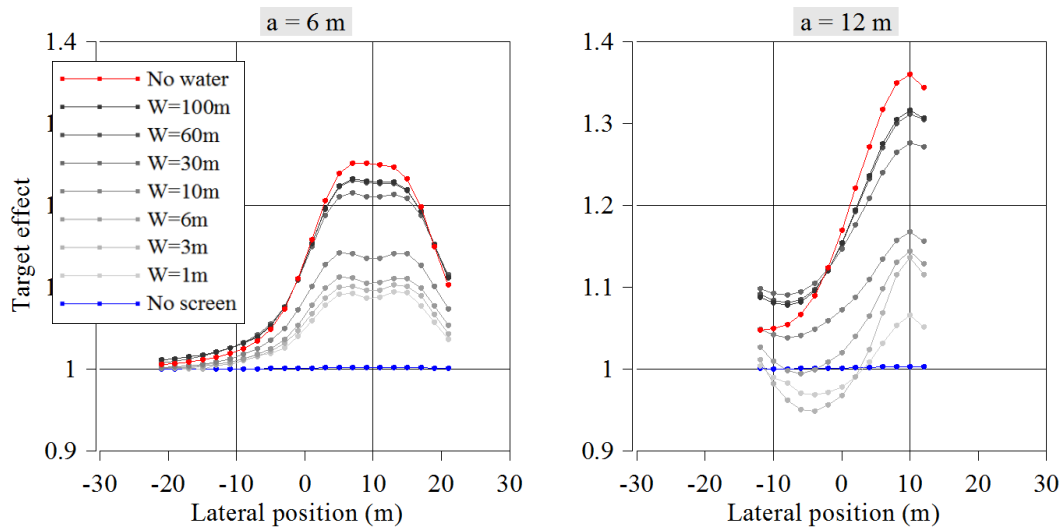


Figure 3 Geological target effect exemplified for two electrode spacings of a Wenner- α array throughout the electrode line and for the 9 screen configurations.

A significant target effect is reached for all electrode spacings (including all those not shown in Figure 3) even for values of $W < L/2$. This gives room for finding a trade-off between a sufficient target effect and a reasonable screen size. From a more general point of view, it can be anticipated that such a trade-off may highly depend on the geological context and the survey goals. The maximum target effect exhibited by the ‘no water’ configuration, which is the effect one would have on dry land for the same target and same resistivity contrast with the sediments, seems not to be attainable. This is because in this study the sheet size only increases in width and keeps constant in length, whereas an infinite screen in both directions is needed to reach the ‘no water’ response.

Conclusion

We have introduced a straightforward technique for improving marine DC-resistivity acquisitions. The technique is based on the use of an insulating sheet laid directly on the electrode line placed on the seafloor. The effect of such a screen was illustrated by means of numerical modelling and partly validated by comparing simulated data in a homogeneous medium to a well-known analytical solution. A synthetic study in a layered medium was then presented to demonstrate the increase in geological target effect as a function of the sheet width. Although DC-resistivity surveys are often deemed ineffective for seawater depths larger than 10 m when the resistivity contrast between seawater and subsurface is high, our modelling results show that significant target effects can be reached for a seawater column as deep as 30 m. Further research is needed to fully validate the newly introduced acquisition technique and quantify the screening effect in a broader range of situations. Furthermore, for completing the methodology, a dedicated inversion scheme has to be developed for allowing 2D and 3D Electrical Resistivity Imaging in the presence of an insulating sheet. Practical issues will also have to be addressed for assessing the in-situ feasibility.

Acknowledgments

The authors thank Donatienne Leparoux as the leader of the PROSE French project (West Atlantic Marine Energy Center, Région Pays de Loire) that hosted and partly funded the present work.

References

- D'Eu, J.F., Tarits, P., Balem, K., Gaspari, F. and Hautot, S. [2012] An electromagnetic-based streamer for near-shore investigations. *2012 Oceans - Yeosu*, IEEE Conference Proceedings, 1-5.
- Dahlin, T. and Zhou, B. [2004] A numerical comparison of 2D resistivity imaging with 10 electrode arrays. *Geophysical Prospecting*, **52**(5), 379-398.
- Dahlin, T., Loke, M.H., Siikanen, J. and Höök, M. [2014] Underwater ERT survey for site investigation of a new Line for the Stockholm Metro. *20th European Meeting of Environmental and Engineering Geophysics*, Conference Proceedings, 1-5.
- Goto, T., Kasaya, T., Machiyama, H., Takagi, R., Matsumoto, R., Okuda, Y., Satoh, M., Watanabe, T., Seama, N., Mikada, H., Sanada, Y. and Kinoshita, M. [2008] A marine deep-towed DC resistivity survey in a methane hydrate area, Japan Sea. *Exploration Geophysics*, **39**(1), 52-59.
- Lafont, R.J., Lagabrielle, R.J., Côte, P.A. and Pélissier, M. [1991] Procédé et Dispositif de Reconnaissance d'un Sol par Prospection Électrique en Site Aquatique. French Patent FR2650896.
- Lagabrielle, R. [1983] The effect of water on direct current resistivity measurement from sea, river or lake floor. *Geoexploration*, **21**(2), 165-170.
- Tassis, G.A., Tsourlos, P.I. and Rønning, J.S. [2020] Detection and characterization of fracture zones in bedrock in marine environment: possibilities and limitations. *Near Surface Geophysics*, **18**(1), 91-103.